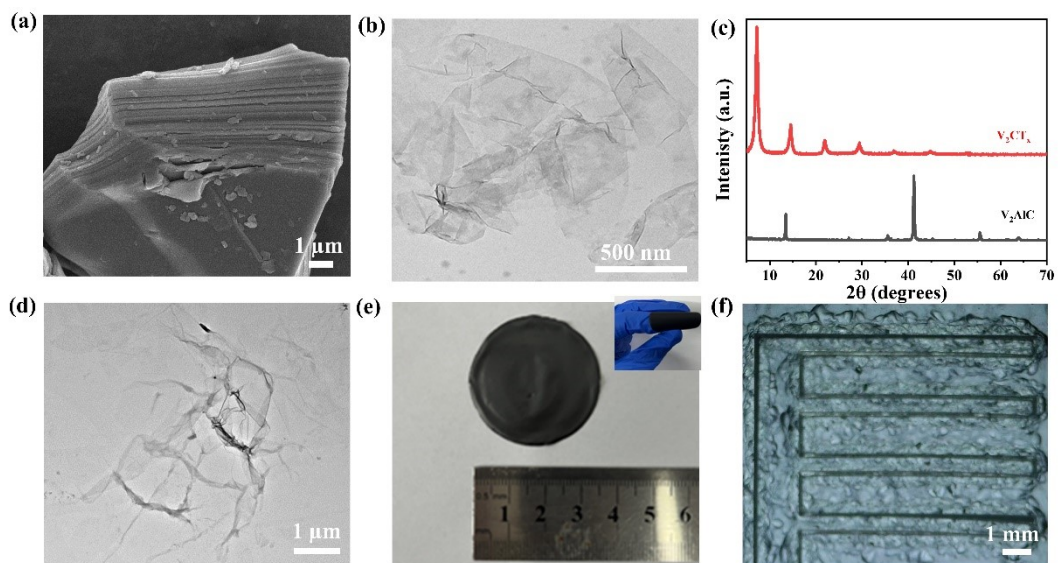


## **Supporting Information**

### **Laser-Assisted Fabrication of a 3D Cross-linked V<sub>2</sub>CT<sub>x</sub>/rGO Microelectrodes for High-Rate Aqueous Zinc-Ion Microbatteries**

Jiao Wu,<sup>a</sup> Long Liu,<sup>a</sup> Cai-Yun Ren,<sup>b</sup> Yong-Chao Zhang,<sup>a</sup> Jian Gao,<sup>\*a</sup> and Xiao-Dong Zhu<sup>\*a</sup>



**Figure S1.** (a) SEM image of the MAX Phase of  $V_2AlC$ . (b) TEM image of the  $V_2CT_x$  flakes. (c) XRD patterns of the MAX phase of  $V_2AlC$  and the  $V_2CT_x$  flakes. (d) TEM image of the GO flakes. (e) Digital photographs of the  $V_2CT_x@GO$  hybrid film and its flexible display. (f) Digital photograph of the interfinger patterned electrode.

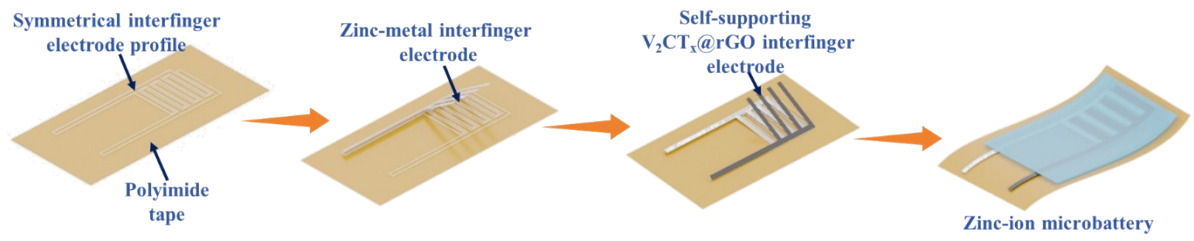


**Figure S2.** The schematic procedure of electrode transfer process.

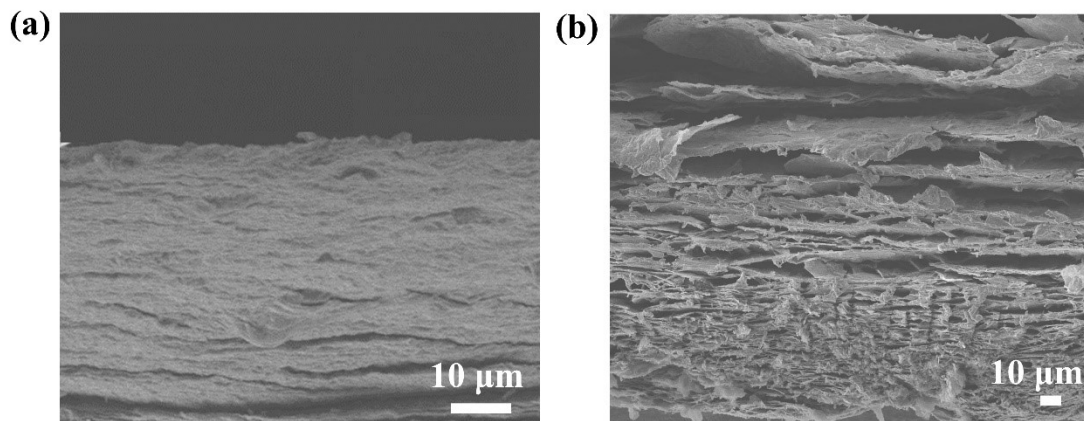


**Figure S3.** (a) SEM image of the 2D  $V_2CT_x@GO$ -60% hybrid film cross section. (b) SEM image of 3D  $V_2CT_x@rGO$ -60% hybrid foam cross section.

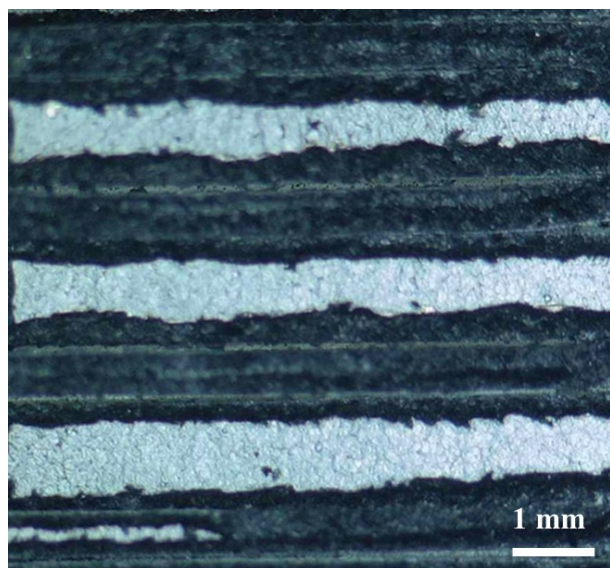


**Figure S4.** The magnification pattern of V<sub>2</sub>CT<sub>x</sub>@rGO-70% interfinger microelectrode

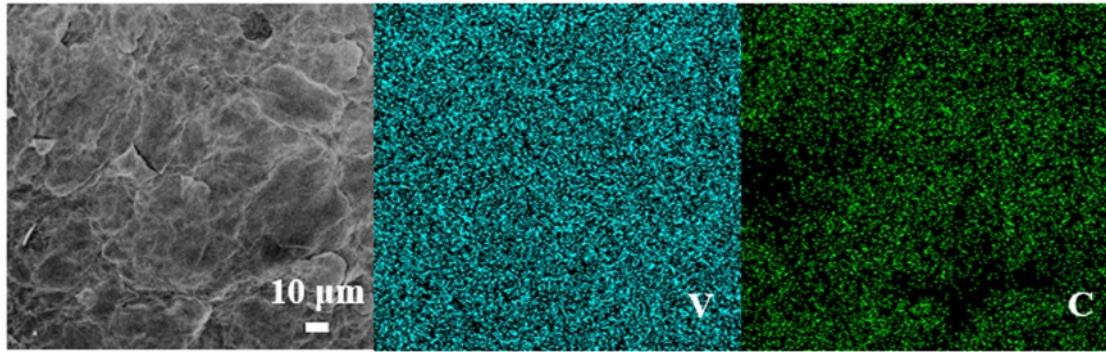


**Figure S5.** The planar SEM image of the 3D hybrid foam and corresponding EDS elemental mapping

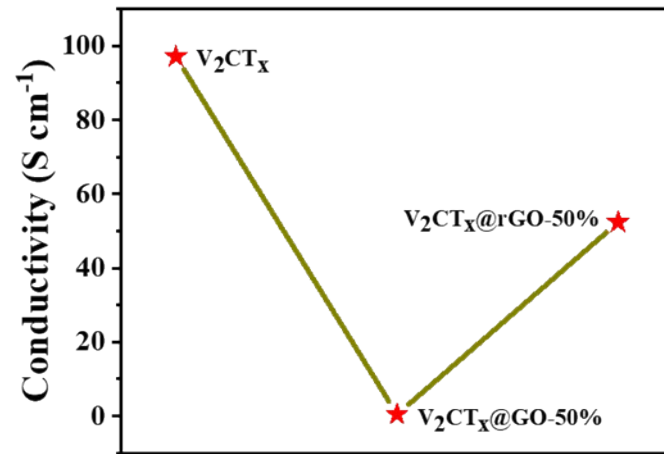


**Figure S6.** The electronic conductivity of the V<sub>2</sub>CT<sub>x</sub>@GO-50%, V<sub>2</sub>CT<sub>x</sub>@rGO-50% and V<sub>2</sub>CT<sub>x</sub>

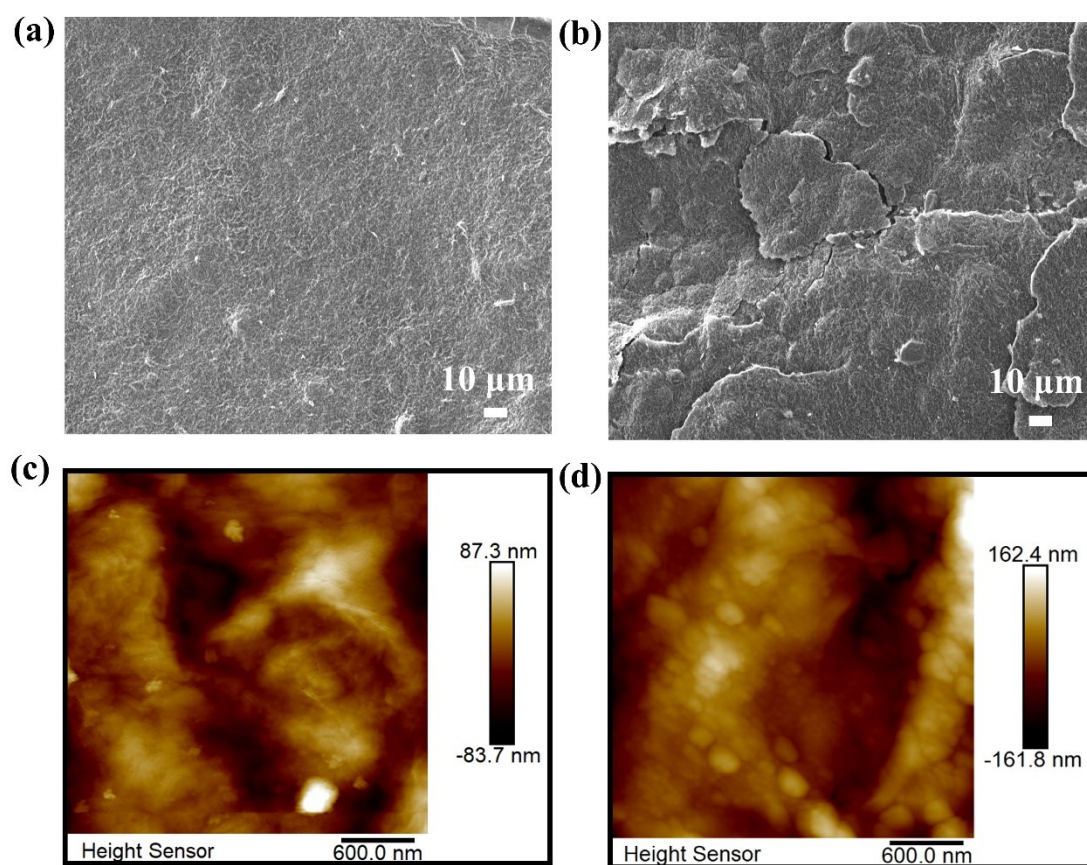


**Figure S7.** (a-b) Planar SEM images of V<sub>2</sub>CT<sub>x</sub>@GO-50% film and V<sub>2</sub>CT<sub>x</sub>@rGO-50% foam. (c-d) Planar AFM images of V<sub>2</sub>CT<sub>x</sub>@GO-50% film and V<sub>2</sub>CT<sub>x</sub>@rGO-50% foam.



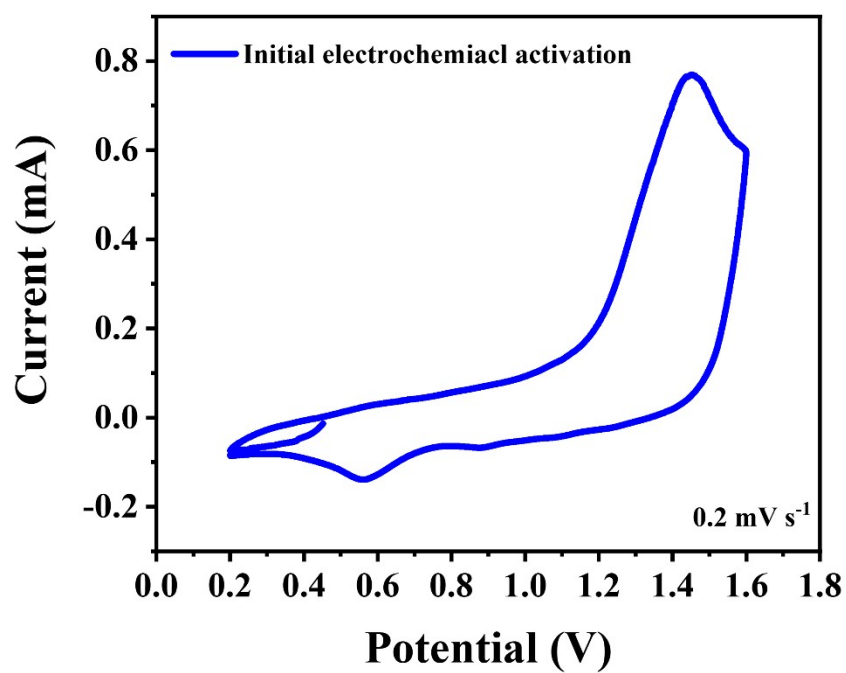


**Figure S8.** CV profile of the initial electrochemical oxidation about 3D VO<sub>x</sub>-V<sub>2</sub>CT<sub>x</sub>@rGO.

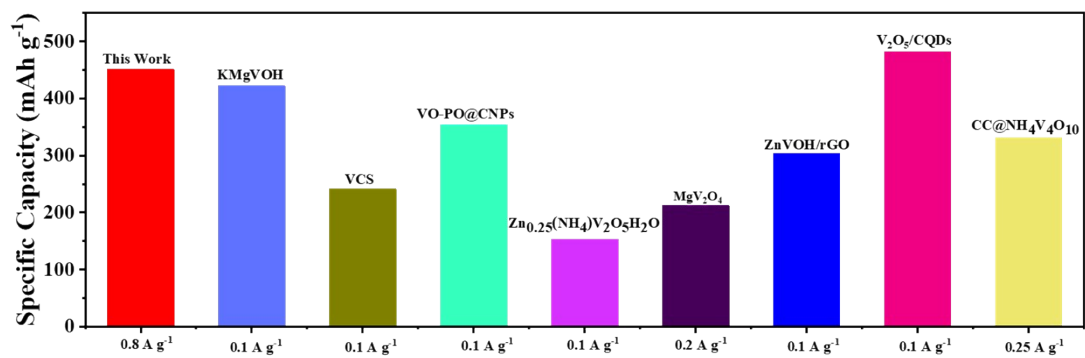


**Figure S9.** The performance comparison bar charts for specific capacity

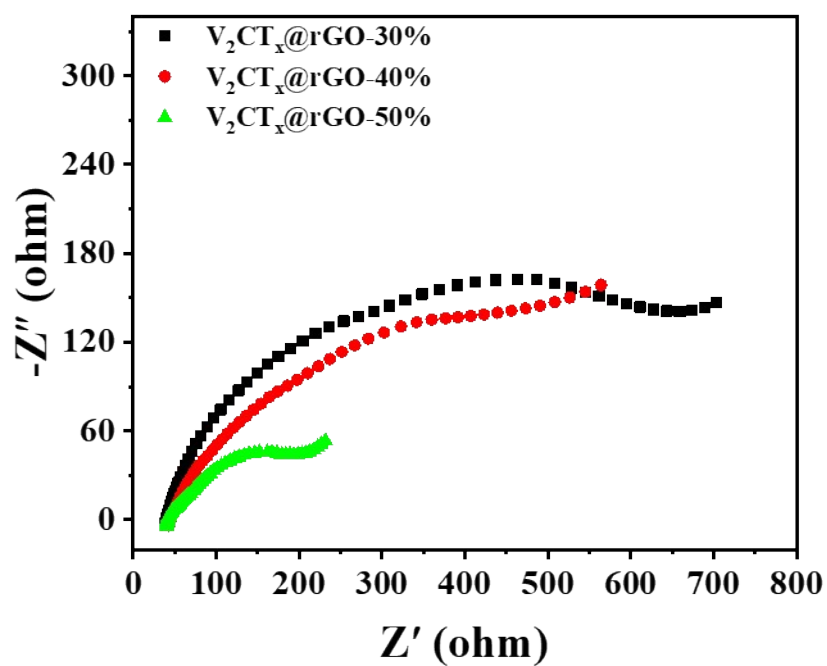


**Figure S10.** The electrochemical impedance spectroscopy (EIS) measured with 3D  $V_2CT_x@rGO-50\%/40\%/30\%$  microelectrodes

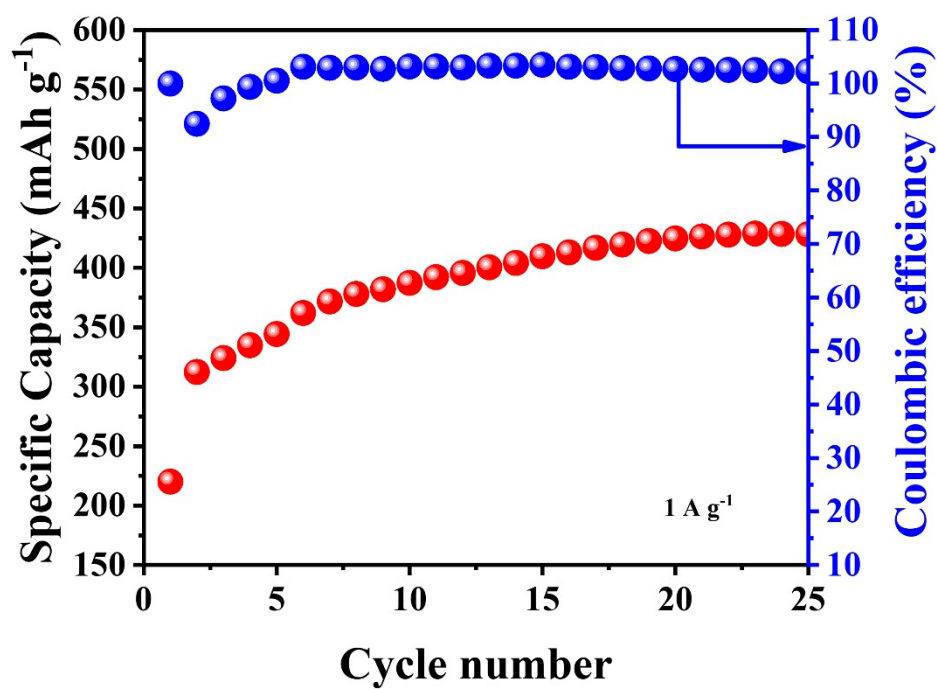


**Figure S11.** Shorter cycle performance and the corresponding Coulombic efficiency at 1 A g<sup>-1</sup> for up to 25 cycles.

**Table S1.** The performance comparison with other microbatteries

Cathode materials	Power density ( $\mu\text{W cm}^{-2}$ )	Energy density ( $\mu\text{Wh cm}^{-2}$ )	Ref
$\text{V}_2\text{O}_5@\text{CNTs}$	193	112.5	[39]
PANI	99	31	[42]
PANI	990	250	[44]
$\text{MnO}_x/\text{polypyrrole}$	178.8	50	[41]
$\text{VO}_2(\text{B})\text{-MWCNTs}$	88.61	124.2	[8]
$\text{MnO}_2@\text{VG}$	67.16	201.5	[40]
$\text{MnO}_2/\text{CNT}$	-	154.6	[43]
KMO/rGO	-	244	[45]
(This work)	615.8	353.54	

